Carbohydrate Polymers 91 (2013) 348–355

Contents lists available at SciVerse ScienceDirect

Carbohydrate Polymers

journal homepage: www.elsevier.com/locate/carbpol

Green, microwave-assisted synthesis of silver nanoparticles using bamboo hemicelluloses and glucose in an aqueous medium

Hong Peng[a,b], Anshu Yang[a,*], Jianghua Xiong[c]

[a] State Key Laboratory of Food Science and Technology, Nanchang University, Nanchang 330047, China
[b] Engineering Research Center for Biomass Conversion, Ministry of Education, Nanchang University, Nanchang 330047, China
[c] Jiangxi Province Agro-Environmental Monitoring Station, Nanchang 330046, China

ARTICLE INFO

Article history:
Received 30 June 2012
Received in revised form 30 July 2012
Accepted 20 August 2012
Available online 25 August 2012

Keywords:
Silver nanoparticles
Hemicelluloses
Glucose
Microwave
Aqueous medium

ABSTRACT

A green, straightforward, microwave-assisted method of synthesizing silver nanoparticles in an aqueous medium was developed using bamboo hemicelluloses as stabilizer and glucose as reducer. The effects of irradiation time as well as initial concentrations of hemicelluloses, glucose, and $AgNO_3$ on the silver nanoparticle formation were studied. The silver nanoparticles were characterized by UV–vis spectroscopy, transmission electron microscopy (TEM), X-ray diffraction (XRD), and X-ray photoelectron spectroscopy (XPS). The results indicated the formation of spherical, nanometer-sized particles. The reaction parameters significantly affected the formation rate, size and distribution of the silver nanoparticles. The average particle size was 8.3–14.8 nm based on TEM analysis. XRD analysis revealed that the particles calcined at 300 °C were face-centered cubic. XPS characterization showed that silver Ag(0) coexisted with silver Ag(I). The synthesis process of silver nanoparticles was rapid and eco-friendly.

1. Introduction

The stabilizing agent, reducing agent, and reaction medium are the three key factors for the efficient synthesis of metal nanoparticles. Stabilizing agents such as thiols (Zhou, Khoury, Qu, Dai, & Li, 2007), triphenylphosphine (Conte, Miyamura, Kobayashi, & Chechik, 2009), polyvinylpyrrolidone (Hou, Dehm, & Scott, 2008), and citrate (Zhang, Li, Goebl, Lu, & Yin, 2011) have been utilized to synthesize metal nanoparticles. However, stabilizers used in the chemical synthesis of metal nanoparticles are often toxic, difficult to dispose, and reduce the utilization of particles. On the other hand, the majority reducing agents reported include sodium borohydride ($NaBH_4$) (Conte et al., 2009; Hou et al., 2008) and hydrogen gas (H_2) (Saliger, Decker, & Prüβe, 2011). All of them are highly reactive and pose potential environmental as well as safety risks. Finally, most synthetic procedures reported rely heavily on organic solvents (Conte et al., 2009; Zhou et al., 2007), inevitably leading to serious environmental problems.

Over the past 10 years, studies have focused on the use of biological compound solutions in synthesizing and stabilizing metal nanoparticles. Biological syntheses of metallic nanoparticles that utilize plant extracts for green synthesis have been extensively carried out (Castro et al., 2011; Gangula et al., 2011; Li, Zhang, Xu, & Zhang, 2011; Vidhu, Aromal, & Philip, 2011). Vidhu et al. (2011) reported the green synthesis of silver nanoparticles using the aqueous seed extract of *Macrotyloma uniflorum*, and the obtained particles have anisotropic morphology and a size of about 12 nm. Some high-potential plant extracts are polyhydroxylated biomacromolecules, such as starch and plant polysaccharides. They present interesting dynamic supramolecular associations facilitated by inter- and intramolecular hydrogen bonding that result in molecular level able to act as templates for nanoparticle growth (Li et al., 2011; Raveendran, Fu, & Wallen, 2003; Vigneshwaran, Nachane, Balasubramanya, & Varadarajan, 2006). Li et al. (2011) developed a new method for constructing silver nanoparticles using triple helical polysaccharide (lentinan) dissolved in water as matrix. The binding interaction between polysaccharides and metal nanoparticles is weak compared with the interaction between typical thiol-based copulating agents and nanoparticles. Thus the stabilizing agent polysaccharides can be easily removed and separated (Raveendran et al., 2003). Several polysaccharides have been evaluated as protecting and capping agents for the preparation of metal nanoparticles (Bilgainya, Khan, & Mann, 2010; Kong, Wong, Gao, & Chen, 2008; Li et al., 2011; Raveendran et al., 2003; Vigneshwaran et al., 2006). However, studies describing the utilization of renewable biomass hemicelluloses are limited. Hemicelluloses are some of the most abundant polymers in plant cells. In a previous study, our laboratory confirmed that hemicelluloses from bamboo (*Phyllostachys pubescens* Mazel) exist as helical chains or random-coil chains in an aqueous solution (Peng, Wang, et al.,

* Corresponding author. Tel.: +86 791 88333816; fax: +86 791 88333281.
E-mail address: yangasxjh@yahoo.com.cn (A. Yang).

0144-8617/$ – see front matter © 2012 Elsevier Ltd. All rights reserved.
http://dx.doi.org/10.1016/j.carbpol.2012.08.073

2012). The bamboo hemicelluloses consist of arabinoxylans, which are rich in hydroxyl groups (Peng, Wang, et al., 2012). Thus, particles are encapsulated by the special structure and the numerous hydroxyl groups.

In the present work, a green, microwave-assisted synthesis of silver nanoparticles was developed. Renewable biomass bamboo hemicelluloses were used as stabilizing agent, nontoxic biochemical glucose was utilized as reducing agent, and distilled water served as reaction medium. The effects of the reaction conditions on the synthesis of silver particles were studied. The obtained particles were analyzed by UV–vis spectroscopy, transmission electron microscopy (TEM), X-ray diffraction (XRD), and X-ray photoelectron spectroscopy (XPS). The advantages of this methodology include the non-requirement of solvents as well as ability of both stabilizing and reducing agents to be produced from renewable biomass.

2. Materials and methods

2.1. Materials

Hemicelluloses were obtained from bamboo (*P. pubescens* Mazel) using the same separation method as that in our earlier paper (Peng, Hu, et al., 2012). The hemicelluloses were sequentially extracted and purified. The fully dried bamboo powder (100 g, 40–100 mesh) was first dewaxed with toluene–ethanol (2:1, v:v, mL/mL) for 6 h in a Soxhlet apparatus. The dewaxed bamboo powder was partially delignified with 0.6% $NaClO_2$ at pH 4.2–4.7 for 2 h at 75 °C under stirring, and holocellulose was obtained. The holocellulose was sequentially treated with hot water (85 °C) for 3 h under stirring. The obtained solid residue was extracted with 2% KOH at 55 °C for 3 h under stirring with the ratio of dry matter to liquor 1:20 (w/v, g/mL), and then filtrated. The pellet was further extracted with 5% NaOH at room temperature for 12 h, and the alkaline filtrate was obtained. The ratio of dry matter to liquor was also 1:20 (w/v, g/mL). After the alkaline filtrate was neutralized to pH 5.5 with acetic acid, the acid filtrate was concentrated at reduced pressure, and the solubilized hemicelluloses were isolated by precipitation in three volumes of 95% ethanol. Finally, the hemicellulose pellet was washed with 70% ethanol and freeze-dried for further use. Silver nitrate ($AgNO_3$) and glucose were analytical reagent grade. The bamboo hemicelluloses were used as stabilizer and glucose was used as reducing agent. All solutions were prepared with deionized water ($R = 18.2\ M\Omega$) that was prepared by ultrafiltration with a Milli-Q water purification system (Millipore, Bedford, MA, USA). All glass wares were thoroughly cleaned with water and dried in an oven.

2.2. Preparation of silver nanoparticles

In a typical preparation, the hemicellulose powder and glucose powder were dispersed in 20 mL aqueous solution containing $AgNO_3$ precursor in a 100 mL beaker. The solution was then irradiated by microwaves at a constant power of 40 W in a microwave oven (Sineo Microwave Chemical Technology Co., Ltd., China). After reaction completion, the solution was immediately cooled down to room temperature. Next, the solution was adjusted to 20 mL by adding a small amount of distilled water to compensate for the loss of water during microwave irradiation before analysis. The reaction dynamics for the formation of silver nanoparticles was systematically investigated by varying the irradiation time from 50 s to 140 s, initial hemicellulose concentration from 0.5 mg/mL to 6.0 mg/mL, glucose concentration from 1.0 mg/mL to 5.0 mg/mL, and $AgNO_3$ concentration from 0.001 mmol/mL to 0.007 mmol/mL.

Representative silver nanoparticles were prepared under the following conditions: 2.0 mg/mL hemicelluloses, 2.0 mg/mL glucose, 0.004 mmol/mL $AgNO_3$, 120 s microwave irradiation time, and calcination at 300 °C for 1 h in air after complete lyophilization. The obtained black powder containing silver and carbon was further characterized by XRD and XPS techniques.

2.3. Characterization

2.3.1. UV–vis spectra

UV–vis absorption spectra were obtained using a LabTech 300563 UV–visible spectrophotometer within the range of 200–600 nm. Before UV–vis measurements, the solutions obtained after irradiation for different times were diluted in five volumes of water (solution:water, 1:5, mL/mL); other solutions were diluted in 10 volumes of water (solution:water, 1:10, mL/mL).

2.3.2. TEM

The morphology and size of the silver nanoparticles were investigated by TEM using a JEM 2010 instrument at an accelerating voltage of 200 kV. The sample for TEM analysis was prepared by placing a drop of silver nanoparticle solution onto a carbon film supported on a copper grid, followed by water evaporation in air at room temperature.

2.3.3. XRD

XRD was recorded on a Bruker D-8 powder X-ray diffractometer using CuKα radiation ($\lambda = 0.15418$ nm) over a 2θ range of 20°–90° with a step size of 0.02°.

2.3.4. XPS

The exposed silver surface species were determined by XPS on an AXIS ULTRA DLD spectrometer with AlKα radiation ($h\nu = 1486.71$ eV) and a spectrometer resolution of energy of 0.48 eV. The peak positions were corrected for sample charging by setting the C 1s binding energy at 284.8 eV. XPS analysis was conducted at 150 W and a pass energy of 16 eV.

3. Results and discussion

Fig. 1A shows the preparations of silver nanoparticles in aqueous medium. After microwave treatment, the solutions became clear without any suspended solid material, indicating that the hemicelluloses were completely dissolved in water. When only hemicelluloses (2.0 mg/mL) or glucose (2.0 mg/mL) were added to the $AgNO_3$ solution (0.004 mmol/mL), the solution remained a colorless salt solution even after irradiation for 120 s. However, after microwave irradiation for 120 s, Ag^+ reduction was visually confirmed because the colorless $AgNO_3$ solution changed to yellow with the simultaneous addition of hemicelluloses (2.0 mg/mL) and glucose (2.0 mg/mL) (Raveendran et al., 2003; Vidhu et al., 2011; Zhang et al., 2011). Due to Mie scattering, the colloidal silver nanoparticles exhibited absorption from 390 to 420 nm (Kleemann, 1993). Thus, the observed typical surface plasmon resonance (SPR) band at about 415 nm (Fig. 1B) further confirmed the formation of silver nanoparticles when both hemicelluloses and glucose were added to the $AgNO_3$ solution (Raveendran et al., 2003). The symmetric plasmon band indicated that the solution did not contain many aggregated particles. The results indicated that hemicelluloses or glucose alone cannot reduce the Ag salt. These phenomena suggested that silver nanoparticles can be synthesized by the combination of bamboo hemicelluloses and biochemical glucose without externally added seed crystallites. Both hemicelluloses and glucose are involved in the reduction process to produce carbohydrate-conjugated silver nanoparticles. These carbohydrate-conjugated silver nanoparticles have potential uses

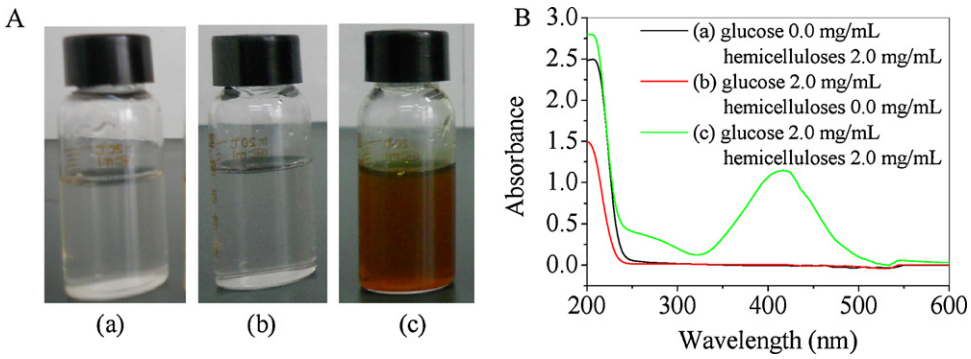

Fig. 1. Photograph of silver particle preparations obtained (A) and corresponding UV–vis spectra (B) with initial precursor $AgNO_3$ 0.004 (mmol/mL) and irradiation time of 120 s ((a) 0.0 mg/mL glucose, 2.0 mg/mL hemicelluloses; (b) 2.0 mg/mL glucose, 0.0 mg/mL hemicelluloses; (c) 2.0 mg/mL glucose and 2.0 mg/mL hemicelluloses).

as antibacterial agents because they are not capped by toxic chemicals. They can also be applied in medicine as well as the textile and pharmaceutical industries. The advantages of using microwave irradiation are the rapid heating rate, ability of uniformly heating the solution, increased reaction kinetics, as well as the formation of a special reaction system that enables selective crystallization and homogeneous nucleation (Kong et al., 2008).

3.1. Effect of reaction parameters on the synthesis of silver nanoparticles

The samples obtained under different microwave irradiation times with 2.0 mg/mL hemicelluloses, 2.0 mg/mL glucose, and 0.004 mmol/mL $AgNO_3$ are shown in Fig. 2. The formation of silver nanoparticles started within 50 s, demonstrating that the reduction reaction was very fast. Interestingly, the sample color gradually changed from colorless to light yellow, yellow, red, and deep red with increased microwave treatment time. The differences among colors of noble metal nanoparticle solutions can depend on the different sizes, shapes, surrounding environment, and structure of particles (Castro et al., 2011; Li et al., 2011). The color change suggested the formation of more silver nanoparticles.

Fig. 3A shows the UV–vis spectra of the silver nanoparticle solutions obtained after irradiation at different times. The strongest SPR band occurred at 415 nm without any shift in the peak wavelength. The maximum absorbance as a function of irradiation time also increased in intensity. These results implied that the silver nanoparticle content increased with increased irradiation time. A new peak as a shoulder also appeared at about 445 nm in the long-wavelength band when the $AgNO_3$ solution containing hemicelluloses and glucose was irradiated for more than 120 s. The appearance of a new peak can be due to the anisotropic nature of the particles (Vidhu et al., 2011). This finding suggested that the size, shape, and surrounding environment of the synthesized silver nanoparticles possibly changed when the solution was microwave irradiated for more than 120 s (Li et al., 2011).

Fig. 3B depicts the UV–vis spectra of the silver nanoparticle solutions obtained with different initial hemicellulose additions. The spectra exhibited unique resonance wavelength at approximately 415 nm, which was associated with the formation of nanoparticles because all their electronic oscillations were equivalent. The absorption peak intensity rapidly increased with increased hemicellulose concentration from 1.0 mg/mL to 2.0 mg/mL. With increased hemicellulose concentration, the increased number of hydroxyl groups facilitated the complexation of Ag^+ to the molecular matrix, whereas the increased number of aldehyde terminals aided the reduction of the same. However, further increased hemicellulose concentration from 4.0 mg/mL to 6.0 mg/mL resulted in decreased the peak intensity, which suggested that the number of particles was reduced. A possible reason was that there was a saturation point between the hemicelluloses and $AgNO_3$, which implied that the concentrated hemicelluloses inhibited the reduction of the $AgNO_3$ precursor, and thus decreased the particle formation rate.

The UV–vis spectra of silver nanoparticle solutions with different initial glucose concentrations are shown in Fig. 3C. The absorption peak was centered at around 413–424 nm for the samples. The SPR band was broader at lower glucose concentrations, indicating the presence of silver nanoparticles with broader size distribution. The absorption peak also became sharper as the amount of glucose increased, and there was a corresponding enhancement in the absorption band intensity.

The effect of $AgNO_3$ concentration on the final silver nanoparticles was also evaluated. Fig. 3D presents the UV–vis spectra of silver nanoparticles synthesized with different initial $AgNO_3$ concentrations by maintaining a constant concentration of 2.0 mg/mL for both hemicelluloses and glucose. Fig. 3D shows that the seven samples exhibited the same maximum absorption peak at 415 nm corresponding to the SPR, and that the peak intensity at 415 nm gradually increased with increased $AgNO_3$ concentration when the concentration ranged from 0.001 mmol/mL to 0.005 mmol/mL. However, a further increase to 0.007 mmol/mL $AgNO_3$ resulted in weaker peak intensity. Therefore, the $AgNO_3$ concentration in solution also affected the shape and size of the formed silver nanoparticles.

3.2. Characterization of the silver nanoparticles

3.2.1. TEM analysis

To understand better the effects of the synthesis conditions on the shape and size of silver nanoparticles, TEM was used to evaluate the morphology and size of some representative silver particles obtained. Fig. 4 presents the TEM images of silver nanoparticles obtained under different conditions. Fewer silver nanoparticles were observed in the solution irradiated for only 50 s (Fig. 4A) than in that irradiated for 120 s (Fig. 4C). Multiple lattice fringes can be clearly observed under high-resolution TEM (Fig. 4B). The lattice spacing of the silver nanoparticles was 0.246 nm, in accordance with the lattice spacing of the {1 0 0} plane of silver (Li et al., 2011; Taleb, Petit, & Pileni, 1997). These results further confirmed the formation of the crystalline nature of the silver nanoparticles. Compared with the preparation containing an initial hemicellulose amount of 2.0 mg/mL (Fig. 4C), the preparation with 6.0 mg/mL hemicelluloses contained much less silver nanoparticles (Fig. 4D). A possible explanation for this phenomenon can be the nanocubic morphology resulting from the slow formation rate of silver particles due to the concentrated hemicellulose concentration. This finding was consistent with the UV–vis analysis results, which showed that the absorption peak intensity of the obtained sample with an initial hemicellulose concentration of 6.0 mg/mL was

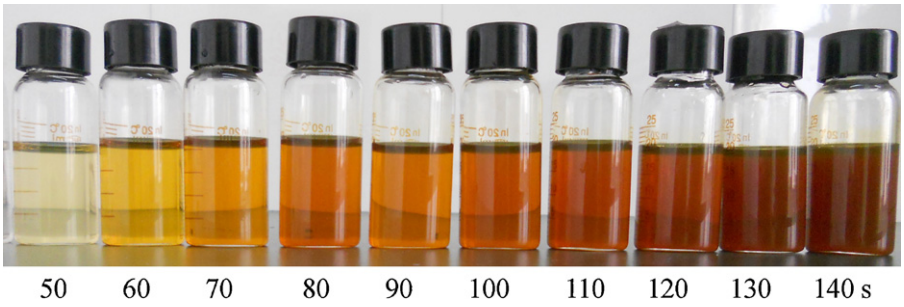

Fig. 2. Photograph of silver nanoparticles obtained after microwave irradiation at different times (2.0 mg/mL hemicelluloses, 2.0 mg/mL glucose, and 0.004 mmol/mL $AgNO_3$).

weaker than that of the obtained sample with 2.0 mg/mL hemicelluloses (Fig. 3B). Obvious aggregation also occurred and resulted in the formation of silver nanoparticles that were larger than 67 nm (Fig. 4E) when a lower amount of glucose was used (1.0 mg/mL). On the other hand, considerably more silver nanoparticles with larger sizes were observed when the silver nitrate concentration was increased to 0.007 mmol/mL (Fig. 4F). The TEM images showed that the silver nanoparticles had better distribution. The shape of the particles was spherical in all TEM images. Both small and large particles were also observed. A possible reason for this result was that during the microwave process, smaller particles transformed with subsequent crystallization into larger particles, which involved the nucleation and growth processes of larger particles from smaller ones (Castro et al., 2011). The silver nanometallic crystals remained within the nanometer-size range possibly because the hemicelluloses prevented the crystals from growing into larger aggregates.

The statistical results are given in Fig. 5 by counting 300 silver nanoparticles in TEM images. Most of the samples presented particle sizes ranging from 4.29 nm to 24.29 nm, except for the sample with an initial glucose concentration of 1.0 mg/mL. When the solution that contained 2.0 mg/mL hemicelluloses, 2.0 mg/mL glucose, and 0.004 mmol/mL $AgNO_3$ was irradiated for 50 s, the obtained silver nanoparticles presented a bimodal distribution that centered at 4.29 and 10.00 nm (Fig. 5A). The number of particles with sizes ranging from 4.29 to 10.00 nm accounted for 75.46%. On the other hand, when the glucose concentration was increased to 2.0 mg/mL, fewer tiny particles (particle size 4.29 nm) formed and the size distribution centered at 11.43 nm (Fig. 5B). Both Fig. 5A and B show that more than 90% of the particles ranged from 4.29 nm to 14.29 nm, implying the possible size selectivity of the template of hemicelluloses. Over 70% of the particles were in the narrow size range from 7.14 to 14.29 nm when the initial hemicellulose concentration was 0.6 mg/mL (Fig. 5C). By comparison, Fig. 5D presents the

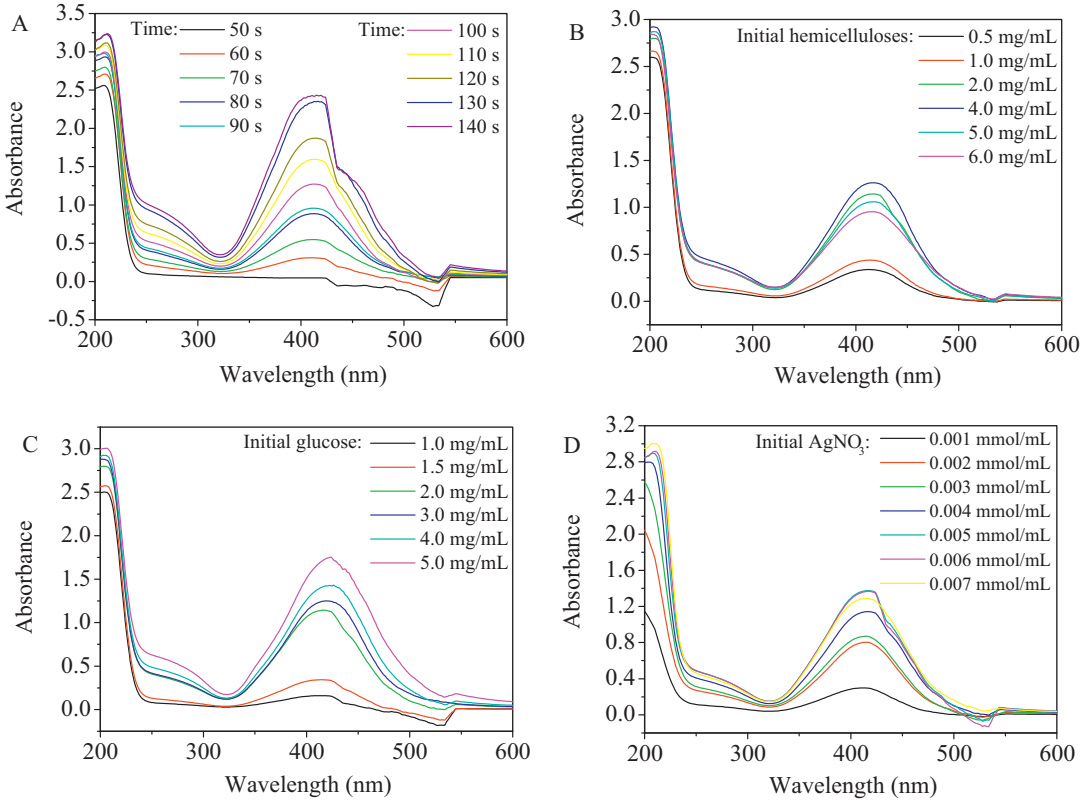

Fig. 3. Effect of reaction parameters on the synthesis of silver nanoparticles: (A) 2.0 mg/mL hemicelluloses, 2.0 mg/mL glucose, 0.004 mmol/mL $AgNO_3$, and irradiation for different times; (B) 2.0 mg/mL glucose, 0.004 mmol/mL $AgNO_3$, irradiation time of 120 s, and different initial hemicellulose amounts; (C) 2.0 mg/mL hemicelluloses, 0.004 mmol/mL $AgNO_3$, irradiation time of 120 s, and different initial glucose amounts; (D) 2.0 mg/mL hemicelluloses, 2.0 mg/mL glucose, irradiation time of 120 s, and different initial $AgNO_3$ concentrations.

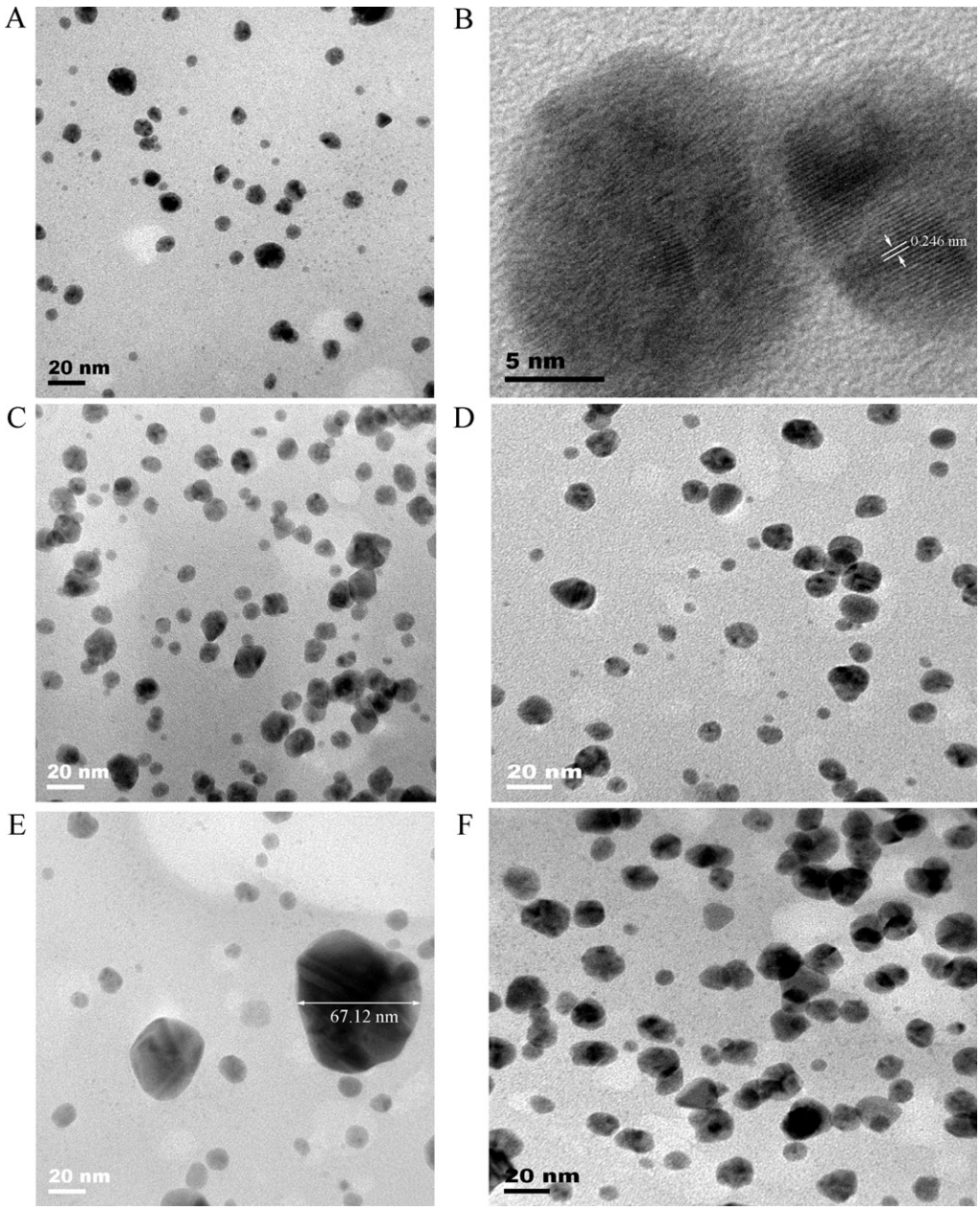

Fig. 4. TEM images of the synthesized silver nanoparticles: (A) 2.0 mg/mL hemicelluloses, 2.0 mg/mL glucose, 0.004 mmol/mL $AgNO_3$, and irradiation time of 50 s; (B) typical high-resolution TEM image of image a; (C) 2.0 mg/mL hemicelluloses, 2.0 mg/mL glucose, 0.004 mmol/mL $AgNO_3$, and irradiation time of 120 s; (D) 6.0 mg/mL hemicelluloses, 2.0 mg/mL glucose, 0.004 mmol/mL $AgNO_3$, and irradiation time of 120 s; (E) 2.0 mg/mL hemicelluloses, 1.0 mg/mL glucose, 0.004 mmol/mL $AgNO_3$, and irradiation time of 120 s; (F) 2.0 mg/mL hemicelluloses, 2.0 mg/mL glucose, 0.007 mmol/mL $AgNO_3$, and irradiation time of 120 s.

widest particle size distribution and appeared to be more polydispersed that the number of particles with size larger than 25 nm, accounting for 10.08%. After the solution containing 2.0 mg/mL hemicelluloses, 2.0 mg/mL glucose, and 0.007 mmol/mL $AgNO_3$ was microwave irradiated for 120 s, the obtained silver particle size centered at 14.29 nm (Fig. 5E). However, compared with Fig. 5B, some particles with sizes larger than 20.00 nm were observed when the initial $AgNO_3$ concentration was increased from 0.004 mmol/mL to 0.007 mmol/mL (Fig. 5E).

Table 1 summarizes the average silver particle sizes obtained from the TEM images. The average particle size of silver nanoparticles obtained with initial glucose concentration 2.0 mg/mL was 9.98 nm, which was much smaller than that of the particles (14.72 nm) produced through reduction by glucose with an initial concentration of 1.0 mg/mL, as indicated in Table 1. The possible reason for this result was that higher concentrations of the reducing agent induced faster nucleation rates that resulted in smaller particle sizes (Kim, Connor, Song, Kuykendall, & Yang, 2004). Increasing the hemicellulose concentration from 2.0 mg/mL to 6.0 mg/mL also resulted in larger average particle sizes. The results of the comparison of silver nanoparticles synthesized by microwave irradiation for 50 s (8.39 nm) and 120 s (9.98 nm) suggested that the size of the silver nanoparticles increased with increased treatment time because of aggregation (Kong et al., 2008). The average particle size of the silver nanoparticles (14.00 nm) was found to be larger at the higher initial $AgNO_3$ concentration of 0.007 mmol/mL. A potential

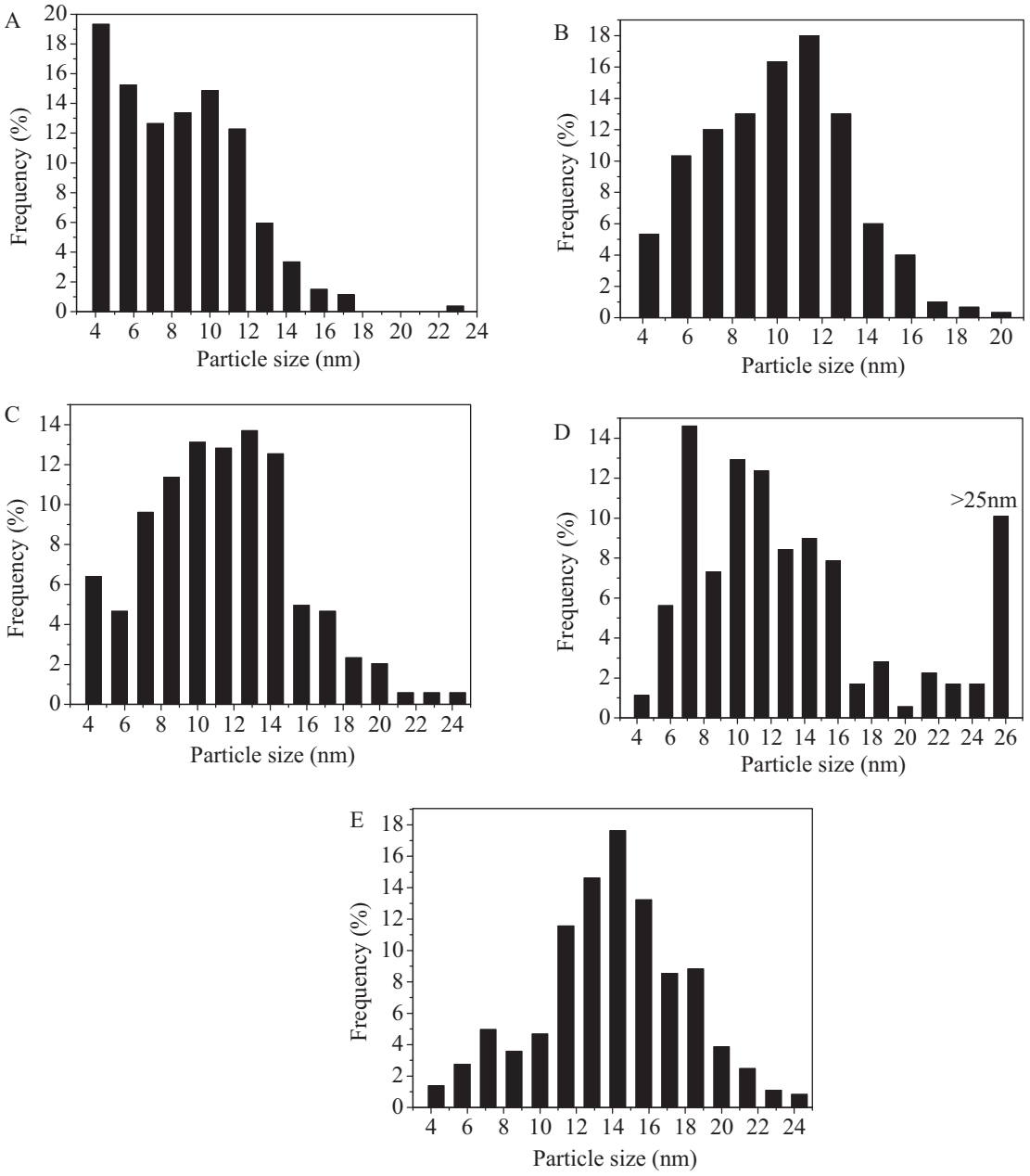

Fig. 5. Histograms of the particle size distribution of silver nanoparticles prepared: (A) 2.0 mg/mL hemicelluloses, 2.0 mg/mL glucose, 0.004 mmol/mL $AgNO_3$, and irradiation time of 50 s; (B) 2.0 mg/mL hemicelluloses, 2.0 mg/mL glucose, 0.004 mmol/mL $AgNO_3$, and irradiation time of 120 s; (C) 6.0 mg/mL hemicelluloses, 2.0 mg/mL glucose, 0.004 mmol/mL $AgNO_3$, and irradiation time of 120 s; (D) 2.0 mg/mL hemicelluloses, 1.0 mg/mL glucose, 0.004 mmol/mL $AgNO_3$, and irradiation time of 120 s; (E) 2.0 mg/mL hemicelluloses, 2.0 mg/mL glucose, 0.007 mmol/mL $AgNO_3$, and irradiation time of 120 s.

reason was that at low initial $AgNO_3$ concentrations, the amount of the stabilizing agent hemicelluloses was sufficient to stabilize the first particles formed in solution. With increased $AgNO_3$ concentration, the silver nanoparticle size also increased because they were not sufficiently capped by hemicelluloses, causing them to become thermodynamically unstable and for aggregates. The TEM analysis showed that the initial hemicellulose concentration, glucose concentration, $AgNO_3$ concentration, and microwave irradiation duration significantly affected the silver particle size and distribution.

Table 1
Sizes of the synthesized silver particles based on TEM images.

Sample	Experimental conditions				Particle size (nm)
	Hemicelluloses (mg/mL)	Glucose (mg/mL)	$AgNO_3$ (mmol/mL)	Time (s)	
A	2.0	2.0	0.004	50	8.39
B	2.0	2.0	0.004	120	9.98
C	6.0	2.0	0.004	120	11.35
D	2.0	1.0	0.004	120	14.72
E	2.0	2.0	0.007	120	14.00

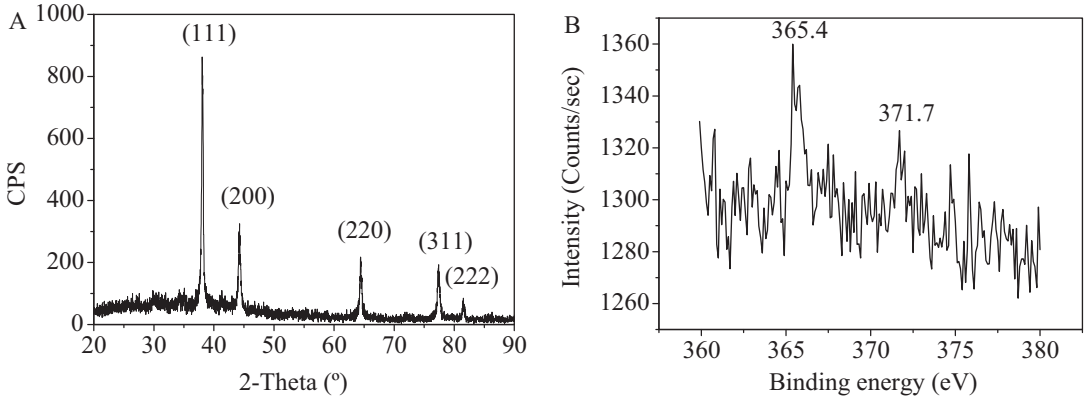

Fig. 6. XRD pattern (A) and XPS spectrum (B) of the silver nanoparticles after thermal treatment at 300 °C for 1 h under air atmosphere.

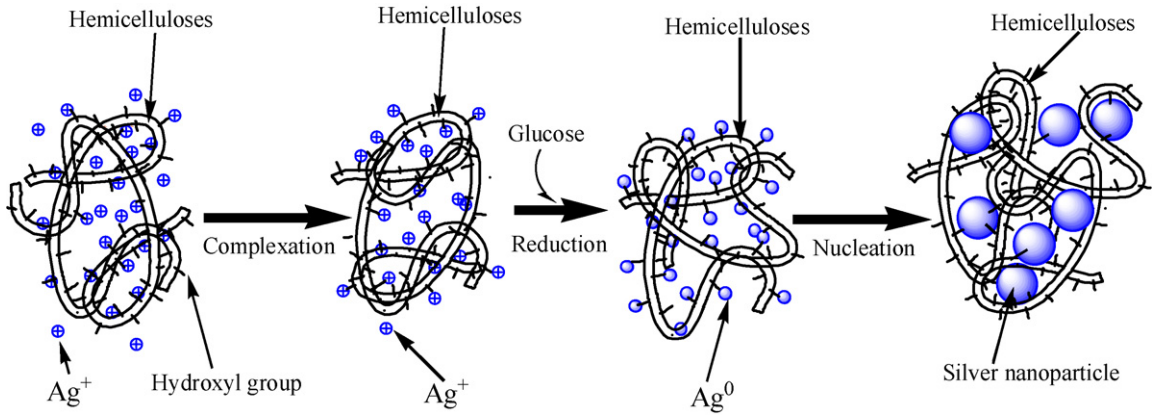

Fig. 7. Schematic illustration of hemicellulose-stabilized silver nanoparticles.

3.2.2. XRD and XPS analyses

The representative silver nanoparticle sample obtained after the solution containing 2.0 mg/mL initial hemicellulose amount, 2.0 mg/mL glucose, and 0.004 mmol/mL $AgNO_3$ was microwave irradiated for 120 s and calcined at 300 °C for 1 h in air after full lyophilization. The formed black powder containing silver and carbon was further analyzed using XRD and XPS techniques. The XRD results are given in Fig. 6A. A typical XRD pattern of the silver nanoparticles with face-centered cubic (fcc) structure had reflections at 38.2° (1 1 1), 44.3° (2 0 0), 64.5° (2 2 0), 77.4° (3 1 1), and 81.6° (2 2 2) (Dubey, Lahtinen, & Sillanpää, 2010; Li et al., 2011). The peak corresponding to the (1 1 1) plane was more intense than the other planes, suggesting that the (1 1 1) plane was in the predominant orientation. From the Debye–Scherrer equation, the average silver particle size was estimated to be 14.52 nm, which was higher than that of the TEM observation result (9.98 nm). A possible reason was that during the thermal treatment at 300 °C for 1 h, agglomeration occurred and resulted in larger silver nanoparticles. However, the silver nanoparticles remained highly nanoscale. The lattice constant calculated from the XRD pattern was 4.0897 Å, in agreement with a previous report (a = 4.086 Å; Joint Committee on Powder Diffraction Standards file no 04-0783).

The XPS spectrum showed double peaks containing a low energy band (Ag $3d_{5/2}$) at 365.4 eV and a higher energy band (Ag $3d_{3/2}$) at 371.7 eV (Fig. 6B). The two peaks can be attributed to the coexistence of the reduction state Ag(0) (binding energy at 365.4 eV) and the oxidation state Ag(I) (binding energy at 371.7 eV) after thermal treatment of the synthesized silver nanoparticles–carbohydrate complex, although the complex was calcined at 300 °C for 1 h in air. The reduced state of Ag (0) had higher content than the oxidized state of Ag (I), as shown by the peak areas in the XPS spectrum.

3.3. Proposed mechanism of silver nanoparticle formation

Hemicelluloses are known to be rich in hydroxyl functional groups. The extensive number of hydroxyl groups in this type of natural hetero-polysaccharides can facilitate the complexation of silver ions to the molecular matrix (Raveendran et al., 2003). Subsequently, these silver ions were reduced to elemental silver by the powerful reducing aldehyde groups of glucose. As a result, these reducing aldehyde groups were oxidized to carbonyl groups. The non-covalent interaction between the hemicellulosic polysaccharides and Ag was stronger than that among the silver nanoparticles themselves (Li et al., 2011). These formed silver nanoparticles can probably be capped and stabilized by the hemicelluloses matrix through the high electronegativity of the hydroxyl groups. This process led to the production of silver particles nanometers in size. The schematic illustration of hemicellulose-stabilized silver nanoparticles is shown in Fig. 7.

4. Conclusion

In this study, a simple and efficient method for the green synthesis of well-distributed spherical silver nanoparticles was developed. The synthesis was carried out in an aqueous medium treated by microwaves using bamboo hemicelluloses as stabilizing agent and glucose as reducing agent. The amounts of hemicelluloses and glucose, as well as the initial $AgNO_3$ concentration and microwave irradiation time had obvious effects on the amount of silver nanoparticles produced and on their average particle sizes and particle size distributions. The average particle sizes of the different preparations were found to range from 8.39 nm to 14.72 nm.

Longer irradiation times led to higher hemicellulose concentrations. Increased $AgNO_3$ concentration corresponded to increased average particle size. Higher glucose concentrations resulted in smaller particle sizes. The utilization of renewable materials such as hemicelluloses and glucose for the synthesis of silver nanoparticles in an aqueous medium offers numerous benefits, including eco-friendliness and compatibility with biomedical, pharmaceutical, and textile applications. Microwave irradiation can accelerate the formation rate of particles.

Acknowledgements

The authors are grateful for financial support of the Natural Science Foundation of China (30960304), of the Key Programme for Bioenergy Industrialization of Jiangxi Provincial Department of Science and Technology (2007BN12100), of the International Science and Technology Cooperation Programme of China (2010DFB63750), of the International Science and Technology Cooperation Programme of Jiangxi Province Department of Science and Technology (2010EHB03200), of the Programme of Jiangxi Provincial Department of Agriculture (2008-66), and of the Research Foundation for Young Scientists of State Key Laboratory of Food Science and Technology (SKLF-QN-201111).

References

Bilgainya, R., Khan, F., & Mann, S. (2010). Spontaneous patterning and nanoparticle encapsulation in carboxymethylcellulos/alginate/dextran hydrogels and sponges. *Materials Science and Engineering C-Materials for Biological Applications*, *30*(3), 352–356.

Castro, L., Blázquez, M. L., Muñoz, J. A., González, F., García-Balboa, C., & Ballester, A. (2011). Biosynthesis of gold nanoparticles using sugar beet pulp. *Process Biochemistry*, *46*(5), 1076–1082.

Conte, M., Miyamura, H., Kobayashi, S., & Chechik, V. (2009). Spin trapping of Au–H intermediate in the alcohol oxidation by supported and unsupported gold catalysts. *Journal of the American Chemical Society*, *131*(20), 7189–7196.

Dubey, S. P., Lahtinen, M., & Sillanpää, M. (2010). Tansy fruit mediated greener synthesis of silver and gold nanoparticles. *Process Biochemistry*, *45*(7), 1065–1071.

Gangula, A., Podila, R., Ramakrishna, M., Karanam, L., Janardhana, C., & Rao, A. M. (2011). Catalytic reduction of 4-nitrophenol using biogenic gold and silver nanoparticles derived from *Breynia rhamnoides*. *Langmuir*, *27*(24), 15268–15274.

Hou, W. B., Dehm, N. A., & Scott, R. W. J. (2008). Alcohol oxidation in aqueous solutions using Au, Pd, and bimetallic AuPd nanoparticle catalysts. *Journal of Catalysis*, *253*(1), 22–27.

Kim, F., Connor, S., Song, H., Kuykendall, T., & Yang, P. D. (2004). Platonic gold nanocrystals. *Angewandte Chemie-International Edition*, *43*(28), 3673–3677.

Kleemann, W. (1993). Random-field induced antiferromagnetic, ferroelectric and structural domain states. *International Journal of Modern Physics B*, *7*(13), 2469–2507.

Kong, J. M., Wong, C. V., Gao, Z. Q., & Chen, X. T. (2008). Preparation of silver nanoparticles by microwave-hydrothermal technique. *Synthesis and Reactivity in Inorganic, Metal-Organic, and Nano-Metal Chemistry*, *38*(2), 186–188.

Li, S., Zhang, Y. Y., Xu, X. J., & Zhang, L. N. (2011). Triple helical polysaccharide-induced good dispersion of silver nanoparticles in water. *Biomacromolecules*, *12*(8), 2864–2871.

Peng, H., Hu, Z. R., Yu, Z. P., Zhang, J. S., Liu, Y. H., Yiqin Wan, Y. Q., & Ruan, R. (2012). Fractionation and thermal characterization of hemicelluloses from bamboo (*Phyllostachys pubescens Mazel*) culm. *Bioresources*, *7*(1), 374–390.

Peng, H., Wang, N., Hu, Z. R., Yu, Z. P., Liu, Y. H., Zhang, J. S., & Ruan, R. (2012). Physicochemical characterization of hemicelluloses from bamboo (*Phyllostachys pubescens Mazel*) stem. *Industrial Crops and Products*, *37*(1), 41–50.

Raveendran, P., Fu, J., & Wallen, S. L. (2003). Completely Green synthesis and stabilization of metal nanoparticles. *Journal of the American Chemical Society*, *125*(46), 13940–13941.

Saliger, R., Decker, N., & Prüβe, U. (2011). D-Glucose oxidation with H_2O_2 on an Au/Al_2O_3 catalyst. *Applied Catalysis B: Environmental*, *102*(3-4), 584–589.

Taleb, A., Petit, C., & Pileni, M. P. (1997). Synthesis of highly monodisperse silver nanoparticles from AOT reverse micelles: a way to 2D and 3D self-organization. *Chemistry of Materials*, *9*(4), 950–959.

Vidhu, V. K., Aromal, S. A., & Philip, D. (2011). Green synthesis of silver nanoparticles using *Macrotyloma uniflorum*. *Spectrochimica Acta Part A: Molecular and Biomolecular Spectroscopy*, *83*(1), 392–397.

Vigneshwaran, N., Nachane, R. P., Balasubramanya, R. H., & Varadarajan, P. V. (2006). A novel one-pot 'green' synthesis of stable silver nanoparticles using soluble starch. *Carbohydrate Research*, *341*(12), 2012–2018.

Zhang, Q., Li, N., Goebl, J., Lu, Z. D., & Yin, Y. D. (2011). A systematic study of the synthesis of silver nanoplates: is citrate a Magic reagent? *Journal of the American Chemical Society*, *133*(46), 18931–18939.

Zhou, X. L., Khoury, J. M. E., Qu, L. T., Dai, L. M., & Li, Q. (2007). A facile synthesis of aliphatic thiol surfactant with tunable length as a stabilizer of gold nanoparticles in organic solvents. *Journal of Colloid and Interface Science*, *308*(2), 381–384.